Phonon mediated off-resonant quantum dot–cavity coupling under resonant excitation of the quantum dot

Arka Majumdar,* Erik D. Kim, Yiyang Gong, Michal Bajcsy, and Jelena Vučković
E. L. Ginzton Laboratory, Stanford University, Stanford, California 94305, USA
(Received 9 April 2011; published 22 August 2011)

We propose a model for phonon-mediated off-resonant quantum dot–cavity coupling and use it to successfully explain recently observed resonant quantum dot spectroscopic results. We explicitly incorporate the effect of phonons, which explains the role of temperature in the coupling mechanism and predicts an asymmetry in the coupling depending on whether the quantum dot is red or blue detuned with respect to the cavity. We show that the off-resonant coupling is enhanced by the cavity; in the absence of such enhancement, the coupling strength is greatly diminished at higher dot-cavity detunings. These results demonstrate that phonon-mediated processes effectively extend the detuning range in which off-resonant QD-cavity coupling may occur beyond that given by pure dephasing processes.

DOI: 10.1103/PhysRevB.84.085309 PACS number(s): 78.67.Hc, 42.50.Pq, 78.67.De

I. INTRODUCTION

One of the interesting recent developments in cavity quantum electrodynamics (CQED) experiments with quantum dots (QDs) coupled to semiconductor microcavities is the observation of off-resonant dot-cavity coupling. This unusual phenomenon has been observed both in photoluminescence studies[1–5] and under resonant excitation of the QD.[6,7] The coupling observed via photoluminescence is attributed to several phenomena including pure QD dephasing,[8] the electron-phonon interactions,[9–12] multiexciton complexes,[13] and charges in the vicinity of the QD.[14] We note that the effect of electron-phonon interactions in cavity QED studies with QDs has been previously studied,[15,16] though not in the context of off-resonant coupling. To isolate the role of phonons in off-resonant QD-cavity coupling, studies employing resonant excitation of the QD are preferable as they avoid possible complications arising from multiexcitonic complexes and nearby charges generated in above band pumping. Though recent experiments were able to affirm the role of phonons in off-resonant coupling by performing photoluminescence measurements, these measurements required site-controlled QDs.[17] Resonant excitation of a QD coupled to an off-resonant cavity has been recently used to perform QD spectroscopy, enabling the observation of power broadening of the QD linewidth and saturation of the cavity emission.[18,19] However, there is presently no theoretical model accounting for off-resonant dot-cavity coupling for the case of resonantly excited QDs. Although off-resonant coupling can be modeled by introducing a phenomenologically incoherent cavity pumping mechanism,[20] such treatment masks the actual physical phenomenon responsible for the coupling. Without an explicit coherent driving term in the system Hamiltonian, the resonant QD spectroscopy results cannot be explained.

In this paper, we theoretically and experimentally investigate off-resonant dot-cavity coupling under resonant excitation of the QD. We first theoretically model the coupling via pure QD dephasing. Then, we propose a model where the phonon-mediated coupling is enhanced by the cavity. We compare these two models and find that they predict qualitatively similar signatures in resonant QD spectroscopic studies, such as power broadening and QD saturation.[18,19] However, in the second model, the coupling is maintained even at very large QD-cavity detunings (∼3 meV). Simulated QD spectroscopy results also exhibit an inherent asymmetry between phonon emission and absorption rate, depending on whether the QD is red or blue detuned from the cavity. To contrast the two theoretical models, we experimentally study several QDs that are off-resonantly coupled to a photonic crystal cavity mode. Analysis of the detuning dependence of the off-resonant coupling shows that pure QD dephasing is incapable of describing experimentally observed results. The phonon-mediated model, on the other hand, provides an intuitive picture that accurately accounts for the persistence of off-resonant coupling at large QD-cavity detunings.

II. THEORY WITH PURE QD DEPHASING

The dynamics of a coherently driven QD (with ground state $|g\rangle$ and excited state $|e\rangle$) coupled to an off-resonant cavity mode is governed by the Hamiltonian H (in a frame rotating at the driving laser frequency):

$$H = \Delta\omega_c a^\dagger a + \Delta\omega_a \sigma^\dagger\sigma + ig(a^\dagger\sigma - a\sigma^\dagger) + \Omega(\sigma + \sigma^\dagger), \tag{1}$$

where a and σ are the annihilation and lowering operators for the cavity mode and the QD, respectively; $\Delta\omega_c = \omega_c - \omega_l$ and $\Delta\omega_a = \omega_a - \omega_l$ are the cavity and dot detunings from the driving laser, respectively; $\Delta = \omega_a - \omega_c$ is the QD-cavity detuning; Ω is the Rabi frequency of the driving laser and is proportional to the laser field amplitude; and g is the coherent interaction strength between the QD and the cavity.

In this coupled system, there are two independent mechanisms for energy dissipation: cavity decay and QD dipole decay. The system losses can be modeled by the Liouvillian, and the master equation describing the dynamics of the lossy system is given by

$$\frac{d\rho}{dt} = -i[H,\rho] + 2\kappa\mathcal{L}[a] + 2\gamma\mathcal{L}[\sigma], \tag{2}$$

where ρ is the density matrix of the coupled QD-cavity system, and 2γ and 2κ are the QD spontaneous emission rate and

 ©2011 American Physical Society

the cavity population decay rate, respectively. We neglect any nonradiative decay of the QD exciton. $\mathcal{L}[D] = D\rho D^\dagger - \frac{1}{2}D^\dagger D\rho - \frac{1}{2}\rho D^\dagger D$ is the Lindblad operator corresponding to a collapse operator D. In addition, phonons in the solid state system destroy the coherence of the exciton. This is generally modeled by adding an additional incoherent decay term $2\gamma_d\mathcal{L}[\sigma^\dagger\sigma]$ to the master equation, where $2\gamma_d$ is the pure dephasing rate of the QD. This term destroys the polarization of the QD without affecting the population of the QD. The dissipation of the QD polarization and population ($\sigma_z = [\sigma^\dagger,\sigma]$) is described by the mean-field equations:

$$\frac{d\langle\sigma\rangle}{dt} = -(\gamma + \gamma_d)\langle\sigma\rangle, \tag{3}$$

$$\frac{d\langle\sigma_z\rangle}{dt} = -2\gamma(1 + \langle\sigma_z\rangle). \tag{4}$$

The linewidth of the QD, at the zero excitation power limit, is $2(\gamma + \gamma_d)$. However, in this model, the effect of phonons is embedded in the phenomenological pure dephasing rate γ_d, which affects only the QD and does not include any cavity effects.

III. THEORY WITH CAVITY-ENHANCED PHONON PROCESS

We now propose a different model for off-resonant dot-cavity coupling, where the phonon-mediated coupling strength is affected by both the cavity and the QD. The effect of phonons can be modeled by adding two additional incoherent decay terms to the master equation. For a blue-detuned QD [Fig. 1(a)] the master equation has the form

$$\frac{d\rho}{dt} = -i[H,\rho] + 2\kappa\mathcal{L}[a] + 2\gamma\mathcal{L}[\sigma] + 2\gamma_r\bar{n}\mathcal{L}(\sigma^\dagger a) + 2\gamma_r(\bar{n}+1)\mathcal{L}(\sigma a^\dagger), \tag{5}$$

where $2\gamma_r$ is the effective decay rate of the QD exciton states via the emission of a phonon and a photon at the off-resonant cavity frequency. $\bar{n}(\Delta,T) = (e^{\hbar\Delta/k_BT} - 1)^{-1}$ is the average number of phonons at the dot-cavity detuning Δ, present in the system at thermal equilibrium with the reservoir at a temperature T (see the appendices). The analysis for a QD red detuned from the cavity [Fig. 1(b)] can be carried out in a similar manner by replacing the final two terms of Eq. (5) with $2\gamma_r\bar{n}\mathcal{L}(\sigma a^\dagger)$ and $2\gamma_r(\bar{n}+1)\mathcal{L}(\sigma^\dagger a)$.

The decay term $\sigma^\dagger a$ denotes the annihilation of a cavity photon and excitation of the QD, while the term $\sigma a^\dagger$ denotes the creation of a cavity photon and collapse of the QD to its ground state. Each process is then accompanied by the creation (or annihilation) of phonons to compensate for the QD-cavity frequency difference. Only the second process is important for observing cavity emission under resonant excitation of the dot. We also note that the observation of QD emission under resonant excitation of the cavity[6] can be modeled in the same way by changing the coherent driving term from $\Omega(\sigma + \sigma^\dagger)$ to $\Omega(a + a^\dagger)$. In this case, the collapse operator $\sigma^\dagger a$ is important. Similar decay channels have been proposed to model cavity assisted atomic decay.[21] We refer to this process as a cavity-enhanced phonon process.

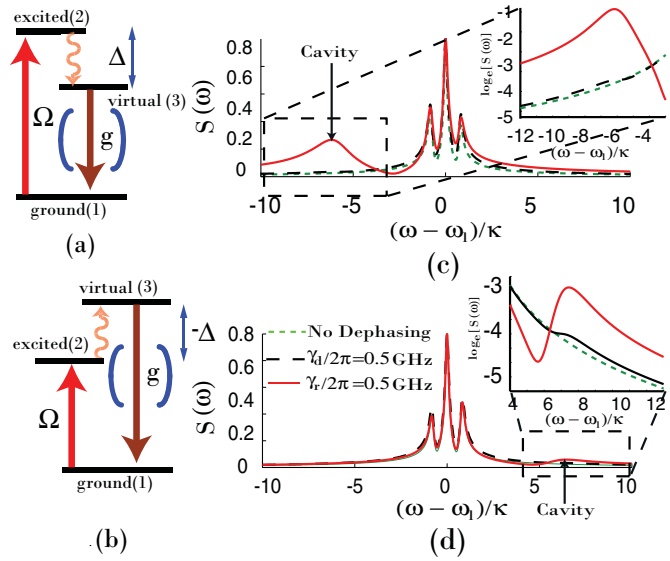

FIG. 1. (Color online) (a), (b) Energy levels of the coupled QD-cavity system where the QD is blue (a) and red (b) detuned from the cavity. A laser drives the quantum dot [transition between ground state (1) and excited state (2)] resonantly. The excited state (2) can decay via two paths: The first is by direct decay back to the ground state (1) via the spontaneous emission; the second is by indirect decay via the emission [Fig. 1(a)] or absorption [Fig. 1(b)] of a phonon [transition (2) to (3)] and subsequent emission of a photon at the cavity frequency [transition (3) to (1)]. (c), (d) Emission $S(\omega)$ as a function of frequency ω for a resonantly driven QD, which is blue (c) and red (d) detuned from the cavity, where ω_l is the laser frequency. Three different cases are considered: without any dephasing, with pure dephasing, and with a cavity-enhanced phonon process. We observe the Mollow triplet at the QD frequency in all three cases. The insets of (c) and (d) show an enlarged view of the emission at the cavity frequency. For the simulation we assume $g/2\pi = \kappa/2\pi = 20$ GHz, $\gamma/2\pi = 1$ GHz, $\Omega/2\pi = 6$ GHz, and QD-cavity detuning $\Delta = \pm 6\kappa$.

We first consider the case where the QD is blue detuned from the cavity [Fig. 1(a)]. The qualitative nature of the dissipation of the QD polarization and population can be determined from the mean-field equations (in the limit $\bar{n} = 0$):

$$\frac{d\langle\sigma\rangle}{dt} = -\gamma\langle\sigma\rangle - \gamma_r(1 + \langle a^\dagger a\rangle)\langle\sigma\rangle, \tag{6}$$

$$\frac{d\langle\sigma_z\rangle}{dt} = -2\gamma(1 + \langle\sigma_z\rangle) - 2\gamma_r(1 + \langle a^\dagger a\rangle)(1 + \langle\sigma_z\rangle). \tag{7}$$

We notice that unlike the pure dephasing case, both the QD population and polarization are affected by the cavity-enhanced phonon process. The linewidth of the QD in the zero excitation power limit is given by $2[\gamma + \gamma_r(1 + \langle a^\dagger a\rangle)]$, which differs qualitatively from the pure QD dephasing model owing to the fact that the presence of cavity photons affects the QD linewidth.

IV. SIMULATION RESULT: POWER BROADENING AND EMISSION SATURATION

The resonance fluorescence of the coupled system is given by the power spectral density (PSD). As we collect the

fluorescence primarily from the cavity, the PSD is calculated as the Fourier transform of the cavity field autocorrelation $S(\omega) = \int_{-\infty}^{\infty} \langle a^\dagger(\tau) a(0) \rangle e^{-i\omega\tau} d\tau$. To determine the two time correlation functions and, subsequently, the PSD, we use the quantum regression theorem.[22]

We simulate the coupled system using numerical integration routines provided in the quantum optics toolbox[23] with realistic system parameters $\kappa/2\pi = g/2\pi = 20$ GHz and $\gamma/2\pi = 1$ GHz. Off-resonant coupling is observed for both strongly ($g > \kappa/2$) and weakly ($g < \kappa/2$) coupled QDs. Figure 1(c) shows numerically calculated resonance fluorescence spectra obtained from the cavity under resonant excitation of a blue detuned QD for three different cases: no dephasing, pure QD dephasing, and no dephasing with a cavity-enhanced phonon process at a bath temperature of 4 K. We first note that no emission is observed at the cavity frequency in the absence of pure dephasing or cavity-enhanced phonon process [see inset of Fig. 1(c)]. Though the pure dephasing ($\gamma_d/2\pi = 0.5$ GHz) and the cavity-enhanced phonon process ($\gamma_r/2\pi = 0.5$ GHz) cases both show off-resonant cavity emission, the latter shows enhanced cavity emission. In all three cases, we also observe the Mollow triplet at the QD frequency, as expected from QD resonance fluorescence.[24] The Mollow sideband closer to the cavity is enhanced causing an asymmetric triplet. Figure 1(d) shows similar spectra for a red-detuned QD. Our model predicts that emission at the cavity frequency is considerably smaller for a red-detuned QD than for a blue-detuned one at finite temperatures, as the process for a red-detuned dot relies on a less-likely phonon absorption and not on phonon emission.

In experimental studies, QD saturation and power broadening have been observed with increasing resonant laser excitation power.[18,19] These phenomena are also observed in our theoretical simulations for both models of off-resonant coupling. We first treat the case of a blue-detuned QD. Figure 2(a) plots the cavity fluorescence as a function of the laser Rabi frequency Ω. For both models, the cavity fluorescence I follows a saturation curve $I = I_{sat}\tilde{P}/(1+\tilde{P})$, where $\tilde{P} \propto \Omega^2$ and I_{sat} is the saturated cavity emission intensity. Figure 2(b) shows the QD linewidth as a function of the laser Rabi frequency Ω. The power broadened QD linewidth $\Delta\omega$ is fitted with the model $\Delta\omega = \Delta\omega_0\sqrt{1+\tilde{P}}$, where $\Delta\omega_0$ is the intrinsic linewidth of the QD and $\tilde{P}$ is obtained from the fit to the saturation of the cavity emission. The theoretical model does not reproduce the additional power-independent broadening of the QD,[18] which results from QD spectral diffusion.[25]

However, the results are dramatically different for a red-detuned QD, as shown in Fig. 3. This is expected because at any temperature, the rates of absorption and emission of phonons are different. We observe that the difference in linewidths of the red- and blue-detuned QD (measured via the off-resonant cavity) is larger, when the QD is weakly driven and hence is not power broadened.[18] This difference reaches the maximum value of $2\gamma_r$ at high temperatures [Fig. 3(a)]. Figure 3(b) shows the ratio of the cavity emission as a function of the bath temperature for different driving laser Rabi frequencies Ω. The difference in cavity emission between a red- and blue-detuned QD is maximum at lower bath temperature and is almost zero at higher temperature.

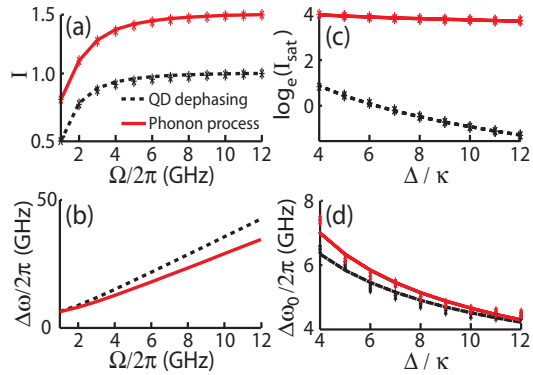

FIG. 2. (Color online) Theoretical resonance fluorescence I collected from the cavity and QD linewidth for a blue-detuned QD ($\Delta > 0$): (a) Normalized cavity fluorescence as a function of the Rabi frequency Ω of the laser for two models. Saturation of the cavity emission is observed. (b) Power broadened QD linewidth (read through the cavity, as in Ref. 18) vs laser Rabi frequency Ω for QD-cavity detuning $\Delta/2\pi = 6$ GHz. (c) Dependence of the saturated cavity emission I_{sat} on the dot-cavity detuning Δ. (d) Dependence of the intrinsic QD linewidth $\Delta\omega_0$ on dot-cavity detuning Δ. $\Delta\omega_0/2\pi$ approaches $2(\gamma+\gamma_d)/2\pi$ or $2(\gamma+\gamma_r)/2\pi$ (both chosen to be 4 GHz) with large Δ. (Parameters used for all the simulations are $\kappa/2\pi = g/2\pi = 20$ GHz and $\gamma/2\pi = 1$ GHz.)

In addition, we investigate the dependence of the saturation emission intensity I_{sat} on the QD-cavity detuning Δ for a blue-detuned dot [Fig. 2(c)]. We note that throughout the paper we fit experimentally measurable quantities with an empirical exponential model $\Delta^{-\alpha}$ to estimate how rapidly the dot-cavity coupling decays as a function of the QD-cavity detuning Δ. This type of model is not valid when the QD is very close to the cavity. However, in experiments this small detuning regime cannot be probed due to large laser background. Also, for very small detunings it cannot be assumed that the laser excites the dot without exciting the cavity, thus complicating the interpretation of experimental results. Results show that I_{sat} falls as $1/\Delta^2$ with the detuning Δ when the dot-cavity coupling is modeled as a pure dephasing process. However, when the coupling is modeled as a cavity-enhanced phonon process,

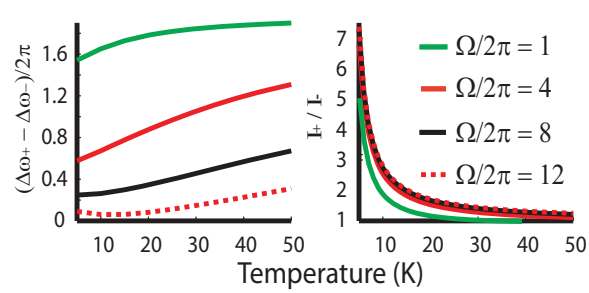

FIG. 3. (Color online) (a) The difference in QD linewidths measured via collected emission through the off-resonant cavity for a blue ($\Delta\omega_+$) and a red ($\Delta\omega_-$) detuned QD for different values of the excitation laser Rabi frequency Ω as a function of the bath temperature T. (b) Ratio of the cavity intensity for an off-resonant QD blue (I_+) and red (I_-) detuned from the cavity as a function of the bath temperature T. For all the simulations, the absolute value of the QD-cavity detuning is kept at 10κ.

the saturation intensity exhibits a much weaker dependence on detuning Δ (estimated to be $\sim 1/\Delta^{0.25}$ for the employed simulation parameters). This signifies an important difference between the two models: The cavity-enhanced phonon process permits observation of off-resonant coupling for a much larger detuning range than that associated with pure dephasing. We also analyze the intrinsic QD linewidth $\Delta\omega_0$ [obtained from Fig. 2(b) at $\Omega = 0$ limit] as a function of the QD-cavity detuning Δ for two different models [Fig. 2(d)]. We observe that at large detuning, $\Delta\omega_0$ approaches the unperturbed QD linewidth $2(\gamma + \gamma_d)$ and $2(\gamma + \gamma_r)$ for the pure dephasing and cavity-enhanced phonon models, respectively. The weak dependence of the intrinsic QD linewidths on the dot-cavity detuning shows that the off-resonant cavity does not perturb the QD significantly.

V. EXPERIMENTAL DATA

We now compare our theoretical model with experimental studies of the cavity emission as a function of QD-cavity detuning Δ for several QDs. Measurements are obtained using the same experimental setup and approach as in Ref. 18. Here, the QD linewidth and off-resonant cavity emission are measured as a function of detuning Δ, where this detuning is varied by varying the sample temperature. Figure 4 shows the saturated cavity intensity as a function of the detuning Δ for different QDs. The excitation laser power is the same for all the detunings for a particular dot. For large detunings ($\Delta/\kappa > 10$), we do not expect significant cavity emission for the case of pure dephasing (which is described by Δ^{-2} dependence), but expect significant emission by the cavity-enhanced phonon model [see Fig. 2(c)]. In our experiment, we observe significant cavity emission for such highly detuned QDs; the cavity emission is fitted well with $\Delta^{-\alpha}$ with $\alpha < 2$. This weaker dependence on detuning is thus more consistent with the description of the off-resonant coupling as a cavity-enhanced phonon process. On the other hand, for QDs with smaller detunings, α is very close to 2 and the role of pure dephasing is evident. We do not observe a significant change in the QD linewidth over the detuning range, due both to the weaker dependence of the linewidth on Δ as predicted by the theory [Fig. 2(d)] and to additional broadening caused by spectral diffusion.

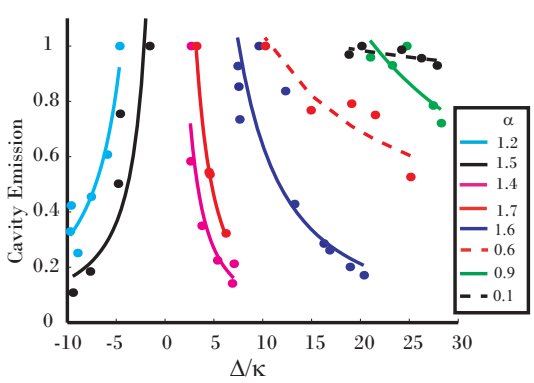

FIG. 4. (Color online) Experimentally observed off-resonant cavity emission as a function of the detuning Δ between the resonantly driven QD and the cavity. Data are fitted with a model $\Delta^{-\alpha}$. Extracted values of α for the different curves are shown.

VI. CONCLUSION

In conclusion, we have compared theoretical treatments of the off-resonant coupling between a resonantly driven QD and a cavity as a pure dephasing process and as a cavity-enhanced phonon process. Comparison with experimental results strongly suggests the role of the cavity-enhanced phonon process in mediating the off-resonant coupling, particularly in the case of large QD-cavity detuning.

While our paper was under review, we became aware of related work[26] analyzing the Mollow triplet in the presence of the off-resonant cavity.

ACKNOWLEDGMENTS

The authors acknowledge financial support provided by the NSF, ARO, and ONR. A.M. acknowledges support from a Stanford Graduate Fellowship (Texas Instruments Fellowship). E.K. acknowledges support from an Intelligence Community (IC) Postdoctoral Research Fellowship.

APPENDIX A: DERIVATION OF DECAY TERMS

We use the level diagram as shown in Fig. 1(a) to model the effect of phonons explicitly. The Hamiltonian of the system is given by

$$H = H_0 + H_I, \tag{A1}$$

where

$$H_0 = \omega_1|1\rangle\langle 1| + \omega_2|2\rangle\langle 2| + \omega_3|3\rangle\langle 3| + \omega a^\dagger a + \sum_j \nu_j b_j^\dagger b_j \tag{A2}$$

and

$$H_I = g_v(a|3\rangle\langle 1| + a^\dagger|1\rangle\langle 3|) + \sum_j g_{23}^j(b_j^\dagger|3\rangle\langle 2| + b_j|2\rangle\langle 3|), \tag{A3}$$

where $|i\rangle\langle i|$ is the population operator for the ith level, a is the annihilation operator for the cavity mode, and b_j is the annihilation operator for a phonon in the jth mode. ω_i, ω, and ν_j are the frequencies of the ith energy level, the cavity resonance, and a phonon in the jth mode. g_v signifies the interaction strength between the cavity and the virtual transition, and g_{23}^j is the interaction strength between the QD exciton and the jth mode phonon. We note that this interaction Hamiltonian is valid only for the level structure as in Fig. 1(a), where the cavity is at lower energy than the QD. For the situation in Fig. 1(b) (where the cavity is of higher energy compared to the QD), the interaction Hamiltonian H_I is given by

$$H_I = g_v(a|3\rangle\langle 1| + a^\dagger|1\rangle\langle 3|) + \sum_j g_{23}^j(b_j|3\rangle\langle 2| + b_j^\dagger|2\rangle\langle 3|). \tag{A4}$$

In the following derivation, we will use the situation shown in Fig. 1(a).

If we define the QD resonance frequency as ω_a, then $\omega_a = \omega_2 - \omega_1$, and the cavity frequency is given by $\omega_c = \omega_3 - \omega_1$.

Then the QD-cavity detuning is given by $\Delta = \omega_2 - \omega_3$. Defining $\sigma_{ij} = |i\rangle\langle j|$, we can write

$$\dot{\sigma_{13}} = -i[\sigma_{13}, H_0 + H_I] = -i\omega_c\sigma_{13} - ig_v a(\sigma_{11} - \sigma_{33}) - i\sum_j g_{23}^j b_j^\dagger \sigma_{12}.$$

Similarly,

$$\dot{\sigma_{23}} = -i[\sigma_{23}, H_0 + H_I] = i\Delta\sigma_{23} - ig_v a\sigma_{21} - i\sum_j g_{23}^j b_j^\dagger(\sigma_{22} - \sigma_{33}).$$

Separating the slow and the fast components of the operators, we can write

$$\sigma_{13} = \tilde{\sigma}_{13}e^{-i\omega_c t}, \tag{A5}$$

$$\sigma_{23} = \tilde{\sigma}_{23}e^{-i\omega_j t}, \tag{A6}$$

$$\sigma_{12} = \tilde{\sigma}_{12}e^{-i(\omega_c-\omega_j)t}, \tag{A7}$$

$$a = \tilde{a}e^{-i\omega_c t}, \tag{A8}$$

$$b_j^\dagger = \tilde{b}_j^\dagger e^{-i\omega_j t}. \tag{A9}$$

Hence the equations governing the dynamics of the system can be written as

$$\dot{\tilde{\sigma}}_{13} = -ig_v\tilde{a}(\tilde{\sigma}_{11} - \tilde{\sigma}_{33}) - i\sum_j g_{23}^j \tilde{b}_j^\dagger \tilde{\sigma}_{12} \tag{A10}$$

and

$$\dot{\tilde{\sigma}}_{23} = i(\Delta - \omega_j)\tilde{\sigma}_{23} - ig_v\tilde{a}\tilde{\sigma}_{21} - i\sum_j g_{23}^j \tilde{b}_j^\dagger(\tilde{\sigma}_{22} - \tilde{\sigma}_{33}). \tag{A11}$$

As level 3 is a virtual level, it is never populated. Hence by adiabatic elimination, using $\dot{\tilde{\sigma}}_{13} = \dot{\tilde{\sigma}}_{23} = 0$, we obtain

$$\tilde{\sigma}_{23} = \frac{g_v\tilde{a}\tilde{\sigma}_{21} + \sum_j g_{23}^j \tilde{b}_j^\dagger(\tilde{\sigma}_{22} - \tilde{\sigma}_{33})}{\Delta - \omega_j} \tag{A12}$$

and

$$\tilde{\sigma}_{12} = \frac{-g_v\tilde{a}(\tilde{\sigma}_{11} - \tilde{\sigma}_{33})}{\sum_j g_{23}^j \tilde{b}_j^\dagger}. \tag{A13}$$

Using these values, we can find the interaction Hamiltonian. The first term $g_v(a\sigma_{31} + a^\dagger\sigma_{13})$ denotes the coherent dynamics. The second term, which signifies the effect of phonons, can be written as [using Eqs. (A12) and (A13)]

$$H_{ph} = \sum_j g_{23}^j(b_j^\dagger\sigma_{32} + b_j\sigma_{23}) \tag{A14}$$

$$= \sum_j g_{23}^j(\tilde{b}_j^\dagger\tilde{\sigma}_{32} + \tilde{b}_j\tilde{\sigma}_{23}) \tag{A15}$$

$$= \sum_j \frac{g_{23}^j g_v}{\Delta - \omega_j}(\tilde{b}_j^\dagger\tilde{a}^\dagger\tilde{\sigma}_{12} + \tilde{b}_j\tilde{a}\tilde{\sigma}_{21}) \tag{A16}$$

$$+ \sum_j \frac{(g_{23}^j)^2}{\Delta - \omega_j}(\tilde{\sigma}_{22} - \tilde{\sigma}_{33})(\tilde{b}_j^\dagger\tilde{b}_j^\dagger + \tilde{b}_j\tilde{b}_j). \tag{A17}$$

The second term involves two-phonon processes which are less likely. If we neglect them, we can model the effect of phonons as follows:

$$H_{ph} = \sum_j \frac{g_{23}^j g_v}{\Delta - \omega_j}(\tilde{b}_j^\dagger\tilde{a}^\dagger\tilde{\sigma}_{12} + \tilde{b}_j\tilde{a}\tilde{\sigma}_{21}). \tag{A18}$$

We can write this Hamiltonian as

$$H_{ph} = (\tilde{a}^\dagger\tilde{\sigma}_{12}\tilde{\Gamma}^\dagger + \tilde{a}\tilde{\sigma}_{21}\tilde{\Gamma}), \tag{A19}$$

where the operator $\tilde{\Gamma}$ can be written as

$$\tilde{\Gamma} = \sum_j \frac{g_{23}^j g_v}{\Delta - \omega_j}\tilde{b}_j \tag{A20}$$

and

$$\Gamma = \sum_j \frac{g_{23}^j g_v}{\Delta - \omega_j} b_j e^{-i\omega_j t}. \tag{A21}$$

To obtain the familiar Lindblad term, we take the partial trace of the correlation between the reservoir operators over the reservoir variables. The correlation is given by

$$\langle\Gamma^\dagger(t')\Gamma(t)\rangle_R = \sum_j \left|\frac{g_{23}^j g_v}{\Delta - \omega_j}\right|^2 e^{-i\omega_j(t-t')}\langle b_j^\dagger b_j\rangle_R. \tag{A22}$$

As the operators b_j are bosonic and the system is in thermal equilibrium with a bath at temperature T, using the relation

$$\langle b_j^\dagger b_j\rangle_R = \bar{n}(\omega_j, T) = \frac{1}{e^{\hbar\omega_j/k_B T} - 1}, \tag{A23}$$

we find

$$\langle\Gamma^\dagger(t')\Gamma(t)\rangle_R = \sum_j \left|\frac{g_{23}^j g_v}{\Delta - \omega_j}\right|^2 e^{-i\omega_j(t-t')}\bar{n}(\omega_j, T) \tag{A24}$$

and

$$\langle\Gamma(t')\Gamma^\dagger(t)\rangle_R = \sum_j \left|\frac{g_{23}^j g_v}{\Delta - \omega_j}\right|^2 e^{-i\omega_j(t-t')}[\bar{n}(\omega_j, T) + 1]. \tag{A25}$$

From the correlation, we find that the phonons with frequency Δ (corresponding to the difference between levels $|2\rangle$ and $|3\rangle$, i.e., QD-cavity mode detuning) have the maximum contribution in the interaction Hamiltonian. In the Born-Markov approximation, we can model the electron-phonon interaction [for Fig. 1(a)] as an incoherent decay process by adding two extra terms to the master equation: $2\gamma_r\bar{n}\mathcal{L}(\sigma^\dagger a)$ and $2\gamma_r(\bar{n}+1)\mathcal{L}(\sigma a^\dagger)$, γ_r being the effective decay rate of the excited QD state and given by

$$\gamma_r = \frac{1}{2}\sum_j \left|\frac{g_{23}^j g_v}{\Delta - \omega_j}\right|^2. \tag{A26}$$

For the situation shown in Fig. 1(b), the decay terms are given by $2\gamma_r\bar{n}\mathcal{L}(\sigma a^\dagger)$ and $2\gamma_r(\bar{n}+1)\mathcal{L}(\sigma^\dagger a)$. We note that the different rates in both cases are due to an inherent asymmetry between the absorption and emission rates of the phonons.

APPENDIX B: DERIVATION OF THE MEAN-FIELD EQUATIONS

To find the mean-field equations for an operator A from the master equation, we used the following relation:

$$\frac{d\langle A\rangle}{dt} = \frac{d}{dt}\mathrm{tr}[A\rho] = \mathrm{tr}\left[A\frac{d\rho}{dt}\right]. \tag{B1}$$

For the cavity-enhanced phonon process, the mean-field equations for a nonzero $\bar{n}$ is given by (when the QD is blue detuned from the cavity)

$$\frac{d\langle\sigma\rangle}{dt} = -\gamma\langle\sigma\rangle - \gamma_r(1+\langle a^\dagger a\rangle)\langle\sigma\rangle + \gamma_r\bar{n}(1+2\langle a^\dagger a\rangle)\langle\sigma\rangle,$$
$$\frac{d\langle\sigma_z\rangle}{dt} = -2\gamma(1+\langle\sigma_z\rangle) - 2\gamma_r(1+\bar{n})(1+\langle a^\dagger a\rangle)(1+\langle\sigma_z\rangle).$$

When the QD is red detuned from the cavity, the mean-field equations are

$$\frac{d\langle\sigma\rangle}{dt} = -\gamma\langle\sigma\rangle - \gamma_r\langle a^\dagger a\rangle\langle\sigma\rangle + \gamma_r\bar{n}(1-2\langle a^\dagger a\rangle)\langle\sigma\rangle,$$
$$\frac{d\langle\sigma_z\rangle}{dt} = -2\gamma(1+\langle\sigma_z\rangle) - 2\gamma_r\bar{n}(1+\langle a^\dagger a\rangle)(1+\langle\sigma_z\rangle).$$

We note that while deriving these mean-field equations, we assume that the cavity and QD operators are uncorrelated and write

$$\langle a^\dagger a\sigma\rangle = \langle a^\dagger a\rangle\langle\sigma\rangle. \tag{B2}$$

Under weak driving, the approximation holds very well. However, in full quantum optical simulations, we do not make any assumptions.

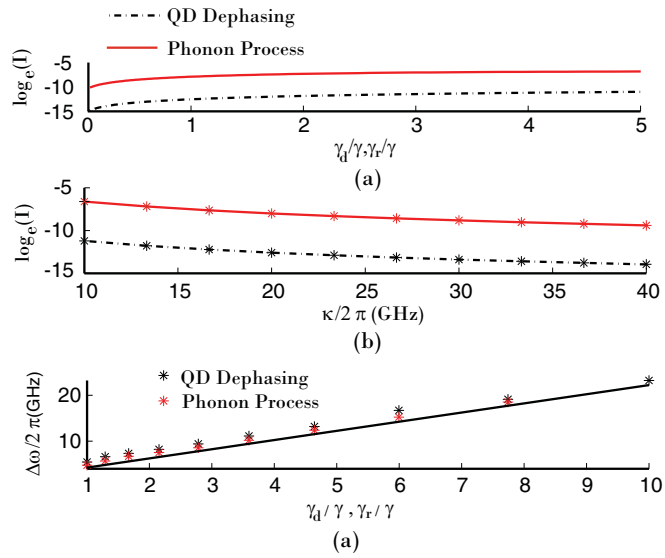

FIG. 5. Resonance fluorescence I collected from the cavity for a blue-detuned QD ($\Delta > 0$). (a) $\log_e(I)$ as a function of the rates γ_d and γ_r (for two models, respectively). $\Delta/\kappa = 10$. (b) $\log_e(I)$ as a function of the cavity linewidth κ, when the dot-cavity detuning $\Delta = 10\kappa$. (c) QD linewidth as a function of the rates γ_d and γ_r for pure dephasing and the cavity-enhanced phonon process, respectively. In both cases, $\Omega/2\pi = 1$ GHz and $\Delta = 12\kappa$. The solid black line shows the theoretical estimates of the QD linewidth when the laser excitation power is very low and the QD is not significantly perturbed by the cavity. (Parameters used for all the simulations are $g/2\pi = \kappa/2\pi = 20$ GHz and $\gamma/2\pi = 1$ GHz.)

APPENDIX C: SIMULATION RESULTS FOR TWO DIFFERENT MODELS: DEPHASING AND CAVITY-ENHANCED PHONON PROCESS

We present more simulation results on the off-resonant cavity emission and QD linewidth by two different models: pure QD dephasing and cavity-enhanced phonon process. We observe that the cavity emission I increases almost linearly with the pure QD dephasing rate γ_d [Fig. 5(a)], but exhibits a nonlinear dependence on the rate γ_r when the coupling is enhanced by the presence of the cavity. Figure 5(b) shows $\log_e(I)$ as a function of the cavity decay rate κ, for a fixed detuning of $\Delta/2\pi = 200$ GHz. For both models, the emission falls off as $1/\kappa^2$, signifying that the off-resonant coupling does not depend on the overlap between the QD and the cavity spectra.

We now measure the QD linewidth $\Delta\omega$ monitoring the cavity emission, while scanning the laser wavelength across the QD resonance, similar to the experiments in Ref. 18. We observe that at very low excitation power $\Omega/2\pi = 1$ GHz and large QD-cavity detuning $\Delta/2\pi = 12\kappa$, the linewidths of the QD are very close to the theoretical linewidth in the absence of the cavity [shown by the solid black line in Fig. 5(c)]. At a constant QD-cavity detuning and laser excitation power, the QD linewidth increases with increasing γ_d and γ_r [Fig. 5(c)].

*arkam@stanford.edu

[1] K. Hennessy, A. Badolato, M. Winger, D. Gerace, M. Atature, S. Gulde, S. Falt, E. L. Hu, and A. Imamoğlu, Nature (London) **445**, 896 (2007).
[2] D. Press, S. Götzinger, S. Reitzenstein, C. Hofmann, A. Löffler, M. Kamp, A. Forchel, and Y. Yamamoto, Phys. Rev. Lett. **98**, 117402 (2007).
[3] M. Kaniber, A. Laucht, A. Neumann, J. M. Villas-Boas, M. Bichler, M.-C. Amann, and J. J. Finley, Phys. Rev. B **77**, 161303 (2008).
[4] D. Dalacu, K. Mnaymneh, V. Sazonova, P. J. Poole, G. C. Aers, J. Lapointe, R. Cheriton, A. J. SpringThorpe, and R. Williams, Phys. Rev. B **82**, 033301 (2010).
[5] A. Laucht, N. Hauke, A. Neumann, T. Günthner, F. Hofbauer, A. Mohtashami, K. Müller, G. Böhm, M. Bichler, M.-C. Amann *et al.*, J. Appl. Phys. **109**, 102404 (2011).
[6] D. Englund, A. Majumdar, A. Faraon, M. Toishi, N. Stoltz, P. Petroff, and J. Vučković, Phys. Rev. Lett. **104**, 073904 (2010).
[7] S. Ates, S. M. Ulrich, A. Ulhaq, S. Reitzenstein, A. Löffler, S. Höfling, A. Forchel, and P. Michler, Nature Photonics **3**, 724 (2009).
[8] A. Auffeves, J.-M. Gerard, and J.-P. Poizat, Phys. Rev. A **79**, 053838 (2009).
[9] Y. Ota, S. Iwamoto, N. Kumagai, and Y. Arakawa, e-print arXiv:0908.0788.

[10]U. Hohenester, Phys. Rev. B **81**, 155303 (2010).
[11]U. Hohenester, A. Laucht, M. Kaniber, N. Hauke, A. Neumann, A. Mohtashami, M. Seliger, M. Bichler, and J. J. Finley, Phys. Rev. B **80**, 201311 (2009).
[12]S. Hughes, P. Yao, F. Milde, A. Knorr, D. Dalacu, K. Mnaymneh, V. Sazonova, P. J. Poole, G. C. Aers, J. Lapointe *et al.*, Phys. Rev. B **83**, 165313 (2011).
[13]M. Winger, T. Volz, G. Tarel, S. Portolan, A. Badolato, K. J. Hennessy, E. L. Hu, A. Beveratos, J. Finley, V. Savona *et al.*, Phys. Rev. Lett. **103**, 207403 (2009).
[14]N. Chauvin, C. Zinoni, M. Francardi, A. Gerardino, L. Balet, B. Alloing, L. H. Li, and A. Fiore, Phys. Rev. B **80**, 241306 (2009).
[15]F. Milde, A. Knorr, and S. Hughes, Phys. Rev. B **78**, 035330 (2008).
[16]I. Wilson-Rae and A. Imamoğlu, Phys. Rev. B **65**, 235311 (2002).
[17]M. Calic, P. Gallo, M. Felici, K. A. Atlasov, B. Dwir, A. Rudra, G. Biasiol, L. Sorba, G. Tarel, V. Savona *et al.*, Phys. Rev. Lett. **106**, 227402 (2011).
[18]A. Majumdar, A. Faraon, E. D. Kim, D. Englund, H. Kim, P. Petroff, and J. Vučković, Phys. Rev. B **82**, 045306 (2010).
[19]A. Ulhaq, S. Ates, S. Weiler, S. M. Ulrich, S. Reitzenstein, A. Löffler, S. Höfling, L. Worschech, A. Forchel, and P. Michler, Phys. Rev. B **82**, 045307 (2010).
[20]F. P. Laussy, E. del Valle, and C. Tejedor, Phys. Rev. B **79**, 235325 (2009).
[21]G. Gangopadhyay, S. Basu, and D. S. Ray, Phys. Rev. A **47**, 1314 (1993).
[22]C. W. Gardiner and P. Zoller, *Quantum Noise* (Springer-Verlag, 2005).
[23]S. M. Tan, J. Opt. B **1**, 424 (1999).
[24]M. O. Scully and M. S. Zubairy, *Quantum Optics* (Cambridge University Press, 2005).
[25]H. Kamada and T. Kutsuwa, Phys. Rev. B **78**, 155324 (2008).
[26]C. Roy and S. Hughes, Phys. Rev. Lett. **106**, 247403 (2011).